

## ■ Medicinal Chemistry &amp; Drug Discovery

# Computational Studies of Selected Transition Metal Complexes as Potential Drug Candidates against the SARS-CoV-2 Virus

Maynak Pal<sup>+</sup>, Dulal Musib<sup>+</sup>, Aniket J. Zade, Neeta Chowdhury, and Mithun Roy<sup>\*[a]</sup>

The earth has witnessed the greatest global health crisis due to the outbreak of the SARS-CoV-2 virus in late 2019, resulting in the pandemic COVID-19 with 3.38 million mortality and 163 million infections across 222 nations. Therefore, there is an urgent need for an effective therapeutic option against the SARS-CoV-2 virus. Transition metal complexes with unique chemical, kinetic and thermodynamic properties have recently emerged as the viable alternative for medicinal applications. Herein, the potential application of selected antiviral transition metal-based compounds against the SARS-CoV-2 virus was explored *in silico*. Initially, the transition metal-based antiviral compounds (1-5) were identified based on the structural similarity of the viral proteins (proteases, reverse transcriptase, envelop glycoproteins, etc.) of HIV, HCV, or Influenza virus with the proteins (S-protein, RNA-dependent RNA polymerase, proteases, etc) of SARS-CoV-2 virus. Hence the complexes (1-5)

were subjected to ADME analysis for toxicology and pharmacokinetics report and further for the molecular docking calculations, selectively with the viral proteins of the SARS-CoV-2 virus. The molecular docking studies revealed that the iron-porphyrin complex (1) and antimalarial drug, ferroquine (2) could be the potential inhibitors of Main protease ( $M_{pro}$ ) and spike proteins respectively of SARS-CoV-2 virus. The complex 1 exhibited high binding energy of  $-11.74$  kcal/mol with the  $M_{pro}$  of SARS-CoV-2. Similarly ferroquine exhibited binding energy of  $-7.43$  kcal/mol against spike protein of SARS-CoV-2. The complex 5 also exhibited good binding constants values of  $-7.67$ ,  $-8.68$  and  $-7.82$  kcal/mol with the spike protein,  $M_{pro}$  and RNA dependent RNA polymerase (RdRp) proteins respectively. Overall, transition metal complexes could provide an alternative and viable therapeutic solution for COVID-19.

## Introduction


The earth has witnessed the most challenging and unprecedented global health crisis of the present century due to the outbreak of the pandemic COVID-19, which is caused by the SARS-CoV-2 virus.<sup>[1]</sup> The pandemic has claimed an estimated 3.38 million mortality with 163 million infections worldwide so far. The SARS-CoV-2 infection is characterized by fever, shortness of breath, loss of appetite and smell, weakness. Acute respiratory distress is the characteristic of later stage SARS-CoV-2 infection.<sup>[2-3]</sup> The respiratory droplets are the common medium of human-to-human infection. Self-isolation of the infected individual, maintaining social distancing, and wearing a face mask are the commonly recommended protocols to prevent the spreading of SARS-CoV-2.<sup>[4-6]</sup> Vaccination against SARS-CoV-2 infection is already rolling over all over the world to prevent SARS-CoV-2 infection. The unknown outcome along with the reduced efficacy of the vaccines against the mutant strains of the SARS-CoV-2 virus is still the area to be worked

out.<sup>[7]</sup> The world health organization (WHO) recommended repurposing selected antiviral/antimalarial drugs e.g. lopinavir, ritonavir, remdesivir, ribavirin or chloroquine/hydroxychloroquine, camostat, nafamostat, bemcentinib, disulfiram, anakinra, canakinumab, sarilumab, tocilizumab, etc. or the combination of multiple antiviral drugs for the treatment of SARS-CoV-2 infection based on the inhibitory potential *in vitro* to the viral proteins of SARS-CoV-2 or interleukins during SARS-CoV-2 infection.<sup>[8-14]</sup> The plasma therapy was also limitedly applied for the treatment of COVID-19.<sup>[15]</sup> The mutations in viral RNA leading to the generation of new mutant strains of SARS-CoV-2, those are more aggressive and more lethal has become very important concerns today and there are no therapeutic options against such aggressive mutant strains of SARS-CoV-2 virus.<sup>[16]</sup> Therefore, the discovery of a specific cure against SARS-CoV-2 is still an elusive goal till now and subject to extensive research.

Although the medicinal chemistry is dominated by carbon-based compounds, but the transition metal complexes with the properties like broad-spectrum of coordination number, geometry, and oxidation number; along with Lewis acid properties and formal charges; kinetic and thermodynamic and properties, tunable redox properties have unfolded them as the potential tools for the medicinal uses.<sup>[17-18]</sup> The complexes of Fe, Ru, Co, Pd, V, Ni, Mn, Zn, Cu, Au, Pt, etc. are reported to exhibit potential antiviral properties against Ebola, Influenza, HIV, and also SARS viruses by the mechanism of interfering with the

[a] M. Pal,<sup>+</sup> D. Musib,<sup>+</sup> A. J. Zade, N. Chowdhury, Dr. M. Roy  
Department of Chemistry  
National Institute of Technology Manipur  
Langol, Imphal West, Pin: 795004  
E-mail: mithunroy@nitmanipur.ac.in

[<sup>+</sup>] These authors contribute equally to the manuscript.

 Supporting information for this article is available on the WWW under <https://doi.org/10.1002/slct.202101852>

primary viral pathogenetic processes, inhibition of the viral entry into the host cells as well as inhibiting the RNA replication process or virus budding processes.<sup>[19–20]</sup> The use of transition metal complexes for antiviral applications is an emerging trend and it becomes very important to explore the potential role of transition metal complexes as the alternative therapeutic option against SARS-CoV-2 and other mutant strains of SARS-CoV-2.<sup>[21–23]</sup>

*In silico* molecular docking has become an important tool to screen transition metal complexes with antiviral properties, as the potential inhibitors against primary viral proteins expressed during viral pathogenesis. There is a remarkable surge in the publication of *in silico* studies related to SARS-CoV-2 indicating the importance of computational evaluation of drug-protein interactions since February 2020.<sup>[24–25]</sup> The recognition of the angiotensin-converting enzyme (ACE2) receptor of the alveolar epithelial host cells by the receptor-binding domain (RBD) of the S2 subunit of the S-protein of the SARS-CoV-2 is the most vital step to initiate the complex viral pathogenesis.<sup>[26–27]</sup>

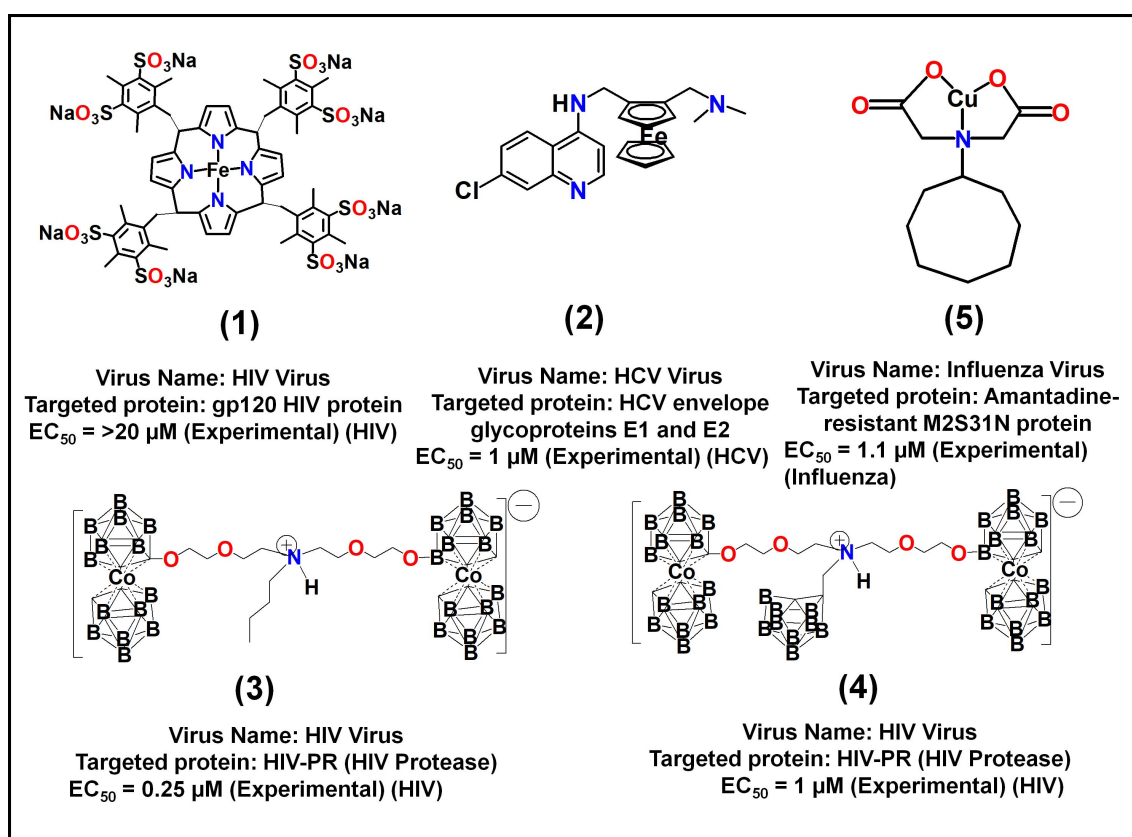
Other viral proteins like RNA-dependent RNA polymerase (RdRp) and M-pro also play an important role in viral replication. Therefore, the receptor-binding domain (RBD) of the Spike protein along with RdRp and  $M_{pro}$  of the SARS-CoV-2 virus offers an ample opportunity for drug design that targets them in preventing the virus to enter into the host cells or replication of the virus.<sup>[28–31]</sup>

Herein, we made a systematic approach to identify the most probable targets proteins (Spike protein, RdRp, and  $M_{pro}$ ) of the SARS-CoV-2 virus by similarity check with the viral proteins of HIV, HCV, Influenza viruses those were targeted by the selected metal-based antiviral complexes (1-5) as reported previously (Scheme 1, Table 1). We have identified and selected only those targets of SARS-CoV-2 that have shown more than 70% structural similarity with the reported proteins of HIV, HCV, Influenza viruses, for the molecular docking studies with the selected transition metal complexes (1-5) (Scheme 1, Table S1).<sup>[31]</sup> Based on the selection, we have carried out in-depth molecular docking studies of the selected metal-based antiviral compounds (1-5) (Scheme 1) with the Spike protein in its receptor-binding domain or  $M_{pro}$  or RNA-dependent RNA polymerase (RdRp) of SARS CoV-2 virus.

## Results and Discussion

### Selection of proteins

Initially we checked the structural similarity of the viral proteins (pro-teases, reverse transcriptase, envelop glycoproteins etc.) of HIV, HCV or Influenza virus with those (Spike glycol protein, proteases, RdRp etc) of the SARS CoV-2 virus (Table S1) and we observed that most of the viral proteins have significant structural resemblance with spike glycoprotein, RNA-dependent RNA polymerase (RdRp) or the  $M_{pro}$  of SARS-CoV-2, those



**Scheme 1.** Selected Metal complexes as antiviral agents considered for molecular docking against different major structural proteins of SARS-CoV-2

**Table 1.** The percentage of structural similarity of different virus (e.g., HIV, HCV, Influenza etc.) vs SARS-CoV-2.

Viruses	Viral Proteins	Protein (SARS-CoV-2)	Structural Similarity	Ref.
HIV and SARS-CoV-2	HIV-PR (HIV Protease) (4TVG)	Spike-glycoprotein (6vxx)	75.76 %	[41]
		Main Protease, M <sub>pro</sub> (6y2g)	53.54 %	
		RNA-dependent RNA Polymerase with RNA (6x2g)	71.72 %	
	HIV-1 RT (5TXM)	Spike-glycoprotein (6vxx)	52.96 %	[37]
		Main Protease, M <sub>pro</sub> (6y2g)	25.85 %	
		RNA-dependent RNA Polymerase with RNA (6x2g)	46.50 %	
	HIV-1 gp 120 (3DNO)	Spike-glycoprotein (6vxx)	84.29 %	[36]
		Main Protease, M <sub>pro</sub> (6y2g)	74.29 %	
		RNA-dependent RNA Polymerase with RNA (6x2g)	82.86 %	
HCV and SARS-CoV-2	HCV envelope glycoprotein E1 (4 N0Y)	Spike-glycoprotein (6vxx)	63.74 %	[39]
		Main Protease, M <sub>pro</sub> (6y2g)	41.56 %	
		RNA-dependent RNA Polymerase with RNA (6x2g)	57.58 %	
	HCV envelope glycoprotein E2 (6MEJ)	Spike-glycoprotein (6vxx)	70.83 %	[26]
		Main Protease, M <sub>pro</sub> (6y2g)	41.74 %	
		RNA-dependent RNA Polymerase with RNA (6x2g)	56.52 %	
Influenza and SARS-CoV-2	Amantadine-resistant M2S31 N protein (Influenza virus) (6MJH)	Spike-glycoprotein (6vxx)	77.78 %	[43]
		Main Protease, M <sub>pro</sub> (6y2g)	70.37 %	
		RNA-dependent RNA Polymerase with RNA (6x2g)	77.41 %	
Dengue and SARS-CoV-2	NS2B/NS3 Protease (Dengue Virus) (4 M9F)	Spike-glycoprotein (6vxx)	58.30 %	–
		Main Protease, M <sub>pro</sub> (6y2g)	39.68 %	
		RNA-dependent RNA Polymerase with RNA (6x2g)	55.47 %	

play a pivotal role during viral attachment and entry into the host cells, replication, and fusion. Targeting and inhibiting those proteins of SARS-CoV-2 virus could be the viable solution for drug design against SARS-CoV-2. We have selected only five metal complexes with antiviral properties from the literatures for the molecular docking studies, those inhibited the proteases, reverse transcriptase, envelop glycoproteins etc. of HIV, HCV or Influenza virus and the proteins have shown structural resembles more than 70% (Table S1). The ADME and toxicology analysis is a very useful computational tool that provides the theoretical pharmacokinetics and toxicology data of compounds that helps to determine the acceptability of the compounds as potential drugs. The selected metal complexes were subjected to ADME analysis to get a fair idea of the compounds in terms of drug acceptability. This analysis is carried out using the webserver SwissADME (<http://www.swissadme.ch/>). However due to the structural complexity the we were unable to generate the smiles id of complex 3 and 4. Hence they were excluded from ADME analysis. Molecular docking, provide us with the various types of molecular interactions that can occur with the target protein and the transition metal complexes and the results potentially could broaden the scope towards understanding the pharmacological aspect in developing metal complexes as potential drugs against SARS-CoV-2.<sup>[32–34]</sup>

In recent years, the application of metalloporphyrin has become very much important in the field of biomedicine such as in PDT for cancer treatment, MRI contrasting agent, anti-viral agent, bio-imaging etc. because of their unique physicochemical properties such as longer wavelength absorption, excellent emission properties, low *in vivo* toxicity, highly singlet oxygen quantum yield etc.<sup>[35]</sup> Here in, we have selected sulphonated anionic Fe-porphyrin complex (1) which showed remarkable anti-HIV (PDB ID: 3DNO)<sup>[36]</sup> with an EC<sub>50</sub> > 20 μM and it also

exhibited anti-HSV activity because it efficiently target the gp120 HIV protein, not CD4 cellular receptor (Scheme 1). The gp120 HIV protein has an 84.29% structural resemblance with the spike glycoprotein of the SARS-CoV-2 virus and we could make fair speculation about the potential interactions of complex 1 with the spike glycoprotein of the SARS-CoV-2 virus. The ADME analysis of the complex 1 reveals that the compound has TPSA (Total polar surface area of 521.71 Å<sup>2</sup>. This indicates the compound has a better chance of forming polar bonds with the amino acid residues of the proteins. The compound also exhibited Consensus Log P<sub>ow</sub> of 5.15 indicating the compound is more soluble in the organic solvent than water. This is due to the large size of the complex 1. The compound also has a very low GI (Gastrointestinal intake) and BBB (blood brain barrier) penetration probability, suggesting for the compound's administration as an intermuscular drug. Molecular docking calculation revealed in the binding energy of –5.95 kcal/mol. The docked pose also exhibits an inhibition constant of 43.22 μM (Table 2) as a result of interaction between the complex 1 and the spike glycoprotein of SARS-CoV-2 virus. There existed a hydrogen bonding interaction along with an electrostatic interaction between the THR548, ARG559, PHE555, LYS553 residues of the spike glycoprotein of SARS-CoV-2 and the complex 1. The H-bonding interaction was between the O atom of the complex and LYS553-H atom, where the complex plays the role of a donor and LYS553 served as an acceptor (Figure 1).

The amino acid sequence of HIV and SARS-CoV-2 main protease (M<sub>pro</sub>) protein was found to be 74.29%. Hence for a better understanding of the inhibition, we have performed molecular docking of complex 1 in the main protease (PDB ID: 6Y2G).<sup>[37]</sup> The best-docked pose revealed remarkable binding energy of –11.74 kcal/mol and inhibition constants of 2.48 nM. There existed five hydrogen bonding interactions along with

**Table 2.** The probable interaction between the complexes and Spike glycol-protein (6VXX), Main Protease,  $M_{\text{pro}}$ (6y2g) and RNA-dependent RNA Polymerase with RNA (6x2g) of SARS-CoV-2.

Complex	Spike glycol-protein (6VXX) <sup>[a]</sup>		Main Protease, $M_{\text{pro}}$ (6y2g) <sup>[a]</sup>		RNA-dependent RNA Polymerase with RNA (6x2g) <sup>[a]</sup>	
	Binding Energy <sup>[b]</sup>	Inhibition constant ( $\mu\text{M}/\text{nM}$ )	Binding Energy <sup>[b]</sup>	Inhibition constant ( $\mu\text{M}/\text{nM}$ )	Binding Energy <sup>[b]</sup>	Inhibition constant ( $\mu\text{M}/\text{nM}$ )
1	-5.95	43.22 $\mu\text{M}$	-11.74	2.48 nM	-7.9	1.61 $\mu\text{M}$
2	-7.43	3.56 $\mu\text{M}$	-	-	-	-
3	-3.29	210 $\mu\text{M}$	-4.32	678.26 $\mu\text{M}$	-	-
4	-2.99	290 $\mu\text{M}$	-	-	-0.13	956.66 $\mu\text{M}$
5	-7.67	2.38 $\mu\text{M}$	-8.68	433.86 nM	-7.82	6.06 $\mu\text{M}$

<sup>[a]</sup> The table contains the details of the interactions between the Spike glycol-protein (6VXX), Main Protease,  $M_{\text{pro}}$ (6y2g) and RNA-dependent RNA Polymerase with RNA (6x2g) of SARS-CoV-2 with the complexes.  
<sup>[b]</sup> The energy values reported in the table contains the unit of kcal/mol.  
<sup>[c]</sup> The binding energy value reported in the table corresponds to the binding free energy ( $\Delta G$ ) of the complex and spike glycol-protein. The other auxiliary factors contributes to the binding energy.]

three hydrophobic interactions between the THR304, ARG4, GLN127, LYS5, VAL125, PRO9, and MET125 residues of the  $M_{\text{pro}}$  of SARS-CoV-2 virus and the complex 1 (Figure 1).

Again, the RNA-dependent RNA polymerase (RdRp) of the SARS-CoV-2 virus has shown 82.86% structural resemblance to the gp120 protein of HIV. Molecular docking calculations, therefore, were performed to probe the inhibitory potential of the complex 1 against RdRp (PDB ID: 6X2G) of the SARS-CoV-2 virus.<sup>[38]</sup> The best docked pose revealed excellent binding energy of -7.9 kcal/mol with the inhibition constants of 1.61  $\mu\text{M}$ .

Also, the docking calculations of complex 1 with the gp 120 HIV protein lead to the binding energy of -9.37 kcal/mol and inhibition constant of 1.02  $\mu\text{M}$  (Figure S1, Table S1).

In the period of 2000–2021, more than 200 research articles were published with interesting results on antimalarial properties of Ferroquine and its derivative. Ferroquine (2) is chloroquine derivative and most active FDA approved organo-metallic drug that is used against malaria.<sup>[39]</sup> Ferroquine (2) can inhibit the HCV RNA replication and could strongly bind to HCV envelope glycoproteins E1 and E2 as well (PDB ID: 4N0Y, 6MEJ)<sup>[40,26]</sup> with an  $\text{IC}_{50}$  value 1.0  $\mu\text{M}$ . The HCV envelope glycoprotein E2 was 70.83% structurally similar to the spike glycoprotein of SARS-CoV-2 virus. The ADME analysis of Ferroquine results in the TPSA of 28.16  $\text{\AA}^2$ . The consensus Log Po/w of Ferroquine is 3.28, indicating moderate water solubility. The compound also has high GI absorption and BBB penetrability that indicates the application of the compound for an oral or intravenous drug. The compound also satisfies the Lipinsky, Ghose, Veber, Egan, and Muegge drug-likeness. All these data correlate with the use of Ferroquine as an effective drug. The molecular docking of the complex 2 into the RBD of the spike glyco-protein complex of SARS-CoV-2 virus revealed the binding energy of -7.43 kcal/mol with an excellent inhibition constant of 3.56  $\mu\text{M}$  (Table 2). There existed two hydrogen bonds, one  $\pi$ -alkyl interaction and one covalent-coordinate bonding interaction between the protein and ferroquine (Figure 2), and the interaction identified were:

(i) N–H (2) and OH (TYR505) (Hydrogen band) (Spike glycol-protein).

(ii) N–H (2) and C=O (GLU37) (Hydrogen band) (Spike glycol-protein).

(iii)  $\pi$ -alkyl interaction between N atom of quinone (2) and HIS34 (RBD, spike protein).

(iv) One covalent coordinate bonding interaction between Fe metal centre (2) and ARG393 (RBD, spike protein).

Similar docking calculation of ferroquine (2) with the HCV envelope glycoprotein E2 exhibited the binding energy of -6.95 kcal/mol with an inhibition constant of 8.1  $\mu\text{M}$  (Figure S2, Table S2).

In past two decades, the use of metallacarboranes (boron cluster) compounds in biomedical field is frequently increased. More than hundreds of boron cluster compounds are reported to exhibit excellent *in vitro* or *in vivo* biological activities including bioimaging, chemotherapeutics, antiviral properties, etc.<sup>[41]</sup> Here in compounds 3 and 4, cobalt(III)-containing B–N cluster complexes and they exhibited significant inhibitory activity against resistant HIV PR variants (PDB ID: 4TVG)<sup>[42]</sup> enzyme. The  $\text{IC}_{50}$  values were reported to be 0.25  $\mu\text{M}$  and 50 nM. The HIV-PR enzyme has shown 75.76% and 82.86% structural resemblance with spike glycoprotein and RNA-dependent RNA Polymerase (RdRp) of the SARS-CoV-2 virus. The molecular docking calculation of complex 3 and 4 with the spike glycoprotein complex of SARS-CoV-2 leads to the binding energy of -3.29 kcal/mol ( $\text{EC}_{50}$ : 210  $\mu\text{M}$ ) and -2.99 kcal/mol ( $\text{EC}_{50}$ : 290  $\mu\text{M}$ ) respectively (Table 2). Though the amino acid sequence of HIV and SARS-CoV-2 main protease and RdRp protein exhibit resembles more than 60%. but molecular docking of complex 3 in the main protease (PDB ID: 6Y2G)<sup>[43]</sup> exhibits lower binding energy of -4.32 kcal/mol (Figure S4). Further investigation of docking interactions of complex 3 with the HIV-PR enzyme revealed the binding energy of -4.04 kcal/mol with an inhibition constant of 356  $\mu\text{M}$  (Figure S5). The binding constant values indicate scope for repurposing of complex 3 as an inhibitor of RdRp protein of SARS-CoV-2. The major molecular interactions contributing to the binding of the complex 3 in the RBD of SARS-CoV-2 spike protein are nine hydrophobic interactions between the complex 3 with LYS378, ALA411, ARG408, VAL407, TYR508 residues of the spike glycoproteins of SARS CoV-2 (Figure S3). Furthermore, the



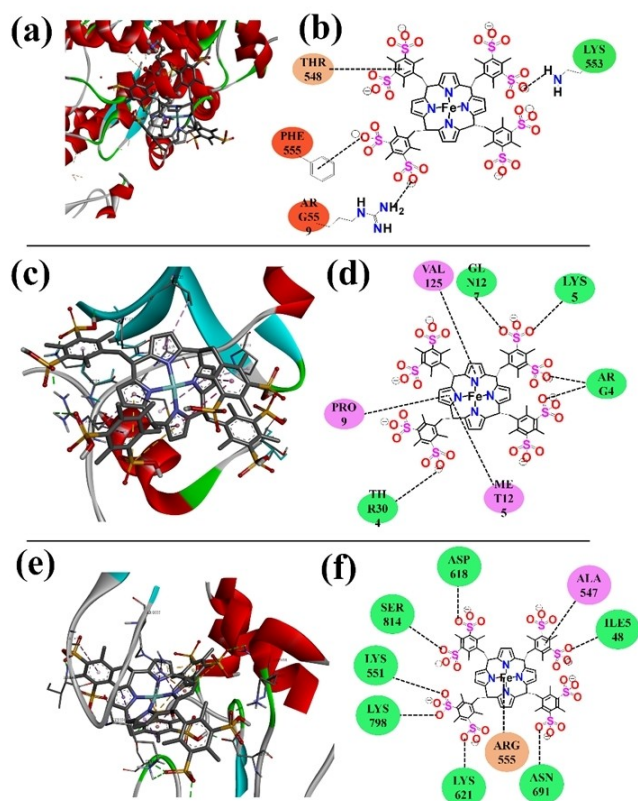


**Figure 1.** (a) The best docked pose of complex 1, that exhibits interactions with the THR548, ARG559, PHE555, LYS553 residues of spike glycoprotein. (b) Schematic representation depicting the most possible non-covalent bonds between the complex 1 and spike glycoprotein of SARS-CoV-2 with the binding site of spike glycoprotein. (H bonding Interactions are: (i) H atom of NH<sub>2</sub>-LYS553 of SARS-CoV-2 spike protein with O6 atom of the complex, (ii) H atom of NH<sub>2</sub>-ARG559 of SARS-CoV-2 spike protein with O15 atom of the complex). (c) The best docked pose of complex 1, that exhibits interactions with the THR304, ARG4, GLN127, LYS5, VAL125, PRO9, and MET125 residues of M<sub>pro</sub>. (d) Schematic representation depicting the most possible non-covalent bonds between the complex 1 and M<sub>pro</sub>-protein of SARS-CoV-2 at the binding site of M<sub>pro</sub>-protein. (Four H-bonding, three hydrophobic interactions) (e) The best docked pose of complex 1, that exhibits interactions with the ASN691, LYS621, LYS798, LYS551, SER814, ASP618, ILE548, ARG555, and ALA547 residues of RdRp. (f) Schematic representation depicting the most possible non-covalent bonds between the complex 1 and RdRp-protein of SARS-CoV-2 at the binding site of RdRp-protein. (seven hydrogen bonding, two hydrophobic interactions).

docked pose of complex 3 in the main protease of SARS-CoV-2 only possesses the weak alkyl-alkyl and alkyl- $\pi$  interaction and leads to a weaker binding interaction. For complex 4, there exist seven hydrophobic interactions between the protein ALA386, ALA387, TYR506 residues of the spike glycoproteins of SARS CoV-2 (Figure S6).

Cyclooctylamine containing copper complex 5 showed excellent blockers of WT (wild type) and the amantadine resistant M2S31 N of influenza virus. The selected copper(II) complex 5 has shown remarkable efficacy against influenza virus (PDB ID: 6MJH),<sup>[44]</sup> and it might target specifically HIS37 in influenza M2. Complex 5 blocked both the WT (wild type) and the amantadine-resistant M2S31 N protein. The EC<sub>50</sub> value was

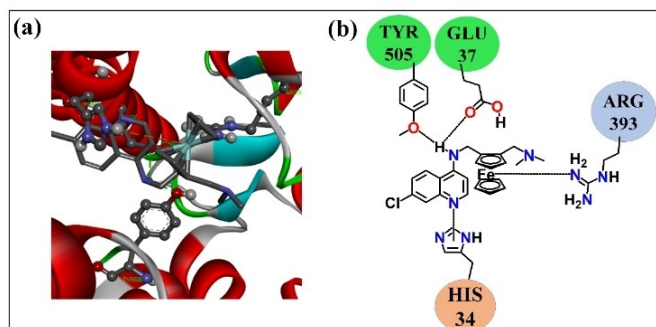


**Figure 2.** (a) The best docked pose of complex 2, that exhibits interactions with the Tyr 505, Glu 37, Arg 393, His 34 residues of spike glycoprotein, (b) Schematic representation depicting the most possible non-covalent bonds between the complex 2 and spike glycoprotein of SARS-CoV-2 in the binding site of spike glycoprotein. (Following Interactions are (i) N–H (2) and OH (Tyr505) (Hydrogen band) (Spike glycoprotein), (ii) N–H (2) and C=O (Glu37) (Hydrogen band) (Spike glycoprotein) (iii)  $\pi$ -alkyl interaction between N atom of quinone and His34, (iv) One covalent coordinate bonding interaction between Fe metal centre and Arg393.

1.1  $\mu$ M in MDCK cells. The amino acid sequence of Influenza virus and SARS-CoV-2 spike glycoprotein was found to be 77.78%. ADME analysis of complex 5 exhibited TPSA of 55.84 Å<sup>2</sup> with consensus Log P<sub>ow</sub> of 1.03. This indicates the good water solubility of complex 5. The compound also exhibits high GI absorption and BBB penetration suggesting the applicability of the complex orally or intravenously. The compound also satisfies all the Lipinski, Ghose, Veber, Egan, and Muegge drug-likeness. All these results suggest the complex 5 as a potent drug for clinical trials. The molecular docking calculation of complex 5 with the spike glycoprotein of SARS-CoV-2 resulted in the binding energy of  $-7.67$  kcal/mol, and the inhibition constant of 2.38  $\mu$ M (Table 2).

There exist three hydrogen bonding and three hydrophobic interactions between the protein and the complex (Figure 3). The major hydrogen bonding interactions are:

- (i) O14 (5) and N–H (LYS562) of spike glycoprotein.
- (ii) O10 (5) and N–H (TRP566) of spike glycoprotein.
- (iii) N7 (5) and N–H (LYS562) of spike glycoprotein.

There were three hydrophobic interactions with PRO565, LAU95, VAL209 residues of the spike glycoprotein, and the complex 5. The amino acid sequence of Influenza virus and SARS-CoV-2 main protease and RdRp protein were found to be 70.37% and 77.41%. Therefore, M<sub>pro</sub> or RdRp of SARS-CoV-2 could be a better target for complex 5. Molecular docking of complex 5 into the main protease (M<sub>pro</sub>) (PDB ID: 6Y2G) revealed the binding energy of  $-8.68$  kcal/mol and inhibition constant of 433.86 nM respectively. The complex afforded to form three hydrogen bonds with the main protease complex of SARS-CoV-2:

- (i) O14 (5) and N–H (ARG4) of Main Protease (M<sub>pro</sub>),
- (ii) O10 (5) and N–H (TRP207) of Main Protease (M<sub>pro</sub>),
- (iii) N6 (5) and H–O (GLU288) of Main Protease (M<sub>pro</sub>).

There was one hydrophobic interaction with complex 5 and Main protease via Phe 291 residue.

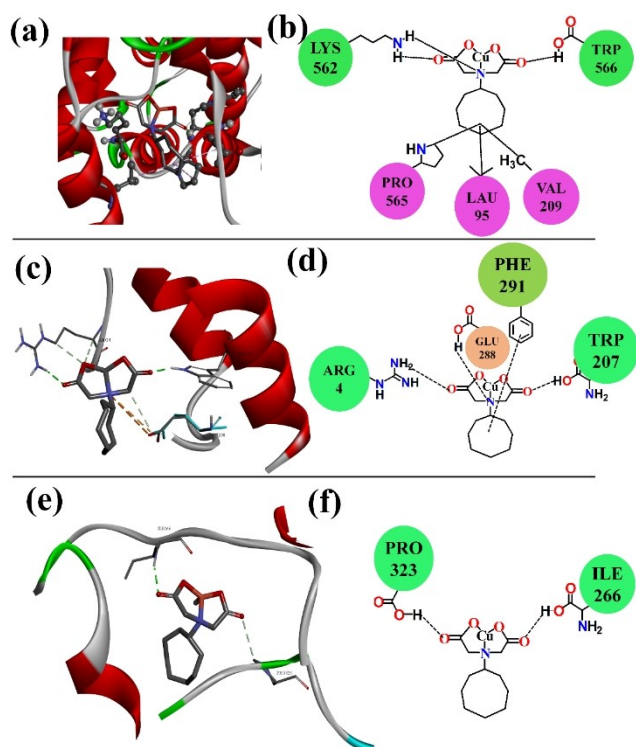


**Figure 3.** (a) The best docked pose of complex 5, that exhibits interactions with the LYS562, PRO565, LAU95, VAL209, TRP566 residues of spike glycoprotein. (b) Schematic representation depicting the most possible non-covalent bonds between the complex 5 and spike glycoprotein of SARS-CoV-2 in the binding site of spike glycoprotein. (Three H-bonding interactions are: (i) O14 (5) and N–H (LYS562) of spike glycoprotein, (ii) O10 (5) and N–H (TRP566) of spike glycoprotein, (iii) N6 (5) and N–H (LYS562) of spike glycoprotein). (c) The best docked pose of complex 5, that exhibits interactions with the ARG4, PHE291, GLU288, TRP207 residues of Main Protease ( $M_{pro}$ ). (d) Schematic representation depicting the most possible non-covalent bonds between the complex 5 and Main Protease ( $M_{pro}$ ) of SARS-CoV-2 in the binding site of  $M_{pro}$ . (Three H-bonding interactions are: (i) O14 (5) and N–H (ARG4) of Main Protease ( $M_{pro}$ ), (ii) O10 (5) and N–H (TRP207) of Main Protease ( $M_{pro}$ ), (iii) N6 (5) and H–O (GLU288) of Main Protease ( $M_{pro}$ )). (e) The best docked pose of complex 5, that exhibits interactions with the PRO323, ILE266 residues of RNA-dependent RNA Polymerase with RNA. (f) Schematic representation depicting the most possible non-covalent bonds between the complex 5 and RdRp of SARS-CoV-2 in the binding site of RdRp. (Two H-bonding interactions are: (i) O14 (5) and N–H (PRO323) of RdRp, (ii) O10 (5) and N–H (ILE266) of RdRp.

Similar docking calculations of the complex 5 with RdRp (PDB ID:6X2G) also revealed strong binding affinity. The best docked poses exhibited binding energy of  $-7.12$  kcal/mol and inhibition constant of  $6.06$   $\mu$ M respectively. The complex afforded to form two hydrogen bonds with the main protease complex of SARS-CoV-2:

- (i) O14 (5) and O–H (PRO323) of RdRp.
- (ii) O10 (5) and O–H (ILE266) of RdRp.

Similar docking of the complex 5 with the WT (wild type) and the amantadine-resistant M2531 N protein revealed the binding energy of  $-6.27$  kcal/mol with an inhibition constant of  $16.56$   $\mu$ M (Figure S7).

## Conclusion

Pandemic COVID-19 resulting from the outbreak of the SARS-CoV-2 virus is the most challenging global health crisis of the present century. Repurposing of current antiviral drugs along with plasma therapy has emerged as the only therapeutic option for COVID-19, although vaccination drive in several countries prevented the viral infection. In addition, the outbreak of other mutant variants of the SARS-CoV-2 virus has made the health crisis more prominent. Therefore, there is an urgent requirement for an effective therapeutic solution against the SARS-CoV-2 virus. Herein, the systematic molecular docking studies with selected, previously reported transition metal-based antiviral agents into the viral proteins of SARS-CoV-2 virus revealed that (i) Fe-porphyrins based complex has emerged as the potential inhibitors of main protease and RNA-dependant RNA polymerase (RdRp). (ii) Ferroquine which is the FDA-approved antimalarial drug, has emerged as the potential inhibitor of spike glycoprotein of SARS-CoV-2 virus. (iii) Copper (II) complex also exhibited remarkable inhibition of spike glycoprotein, main proteases, and RdRp of SARS-CoV-2 virus. The ADME analysis also indicates the drug-likeness of complexes 1, 2, and 5 as potent drugs suitable for clinical trials. Overall, *in silico* studies, herein, explored the potential role of transition metal complexes as the viable and alternative therapeutic solution for COVID-19.

## Supporting Information Summary

Docking energies of the complexes with the SARS-CoV-2 proteins and their initial target proteins, Grid details of molecular docking in the protein structures, Docked pose of complexes with the SARS-CoV-2 target proteins and its other target proteins.

## Acknowledgements

M.R. thank the Board of Research in Nuclear Science (BRNS), Mumbai (37(2)/14/18/2017-BRNS) for funding my research and NIT Manipur for providing infrastructure.

## Conflict of Interest

The authors declare no conflict of interest.

**Keywords:** Antiviral agents · Ferroquine · SARS-CoV-2 virus · Computational chemistry · Molecular docking · Binding energy

- [1] J. Zheng, *Int. J. Biol. Sci.* **2020**, *16*, 1678–1685.
- [2] C. Lai, T. Shih, W. Ko, H. Tang, P. Hsueh, *Int. J. Antimicrob. Agents.* **2020**, *55*, 105924.
- [3] H. Streeck, B. Schulte, B. M. Kümmerer, E. Richter, T. Höller, C. Fuhrmann, E. Bartok, R. Dolscheid-Pommerich, M. Berger, L. Wessendorf, M. Eschbach-Bludau, A. Kellings, A. Schwaiger, M. Coenen, P. Hoffmann, B. Stoffel-Wagner, M. M. Nöthen, A. M. Eis-Hübinger, M. Exner, R. M. Schmithausen, M. Schmid, G. Hartmann, *Nat. Commun.* **2020**, *11*, 5829.
- [4] Y. Ma, E. Frutos-Beltrán, D. Kang, C. Pannecouque, E. D. Clercq, L. Menéndez-Arias, X. Liu, P. Zhan, *Chem. Soc. Rev.* **2021**, *50*, 4514–4540.

- [5] G. E. A. Abuo-Rahma, M. F. A. Mohamed, T. S. Ibrahimcd, M. E. Shomana, E. Samire, R. M. Abd El-Baky, *RSC Adv.* **2020**, *10*, 26895–26916.
- [6] <https://www.who.int/emergencies/diseases/novel-coronavirus-2019/advance-for-public>.
- [7] a) F. Krammer, *Nature* **2020**, *586*, 516–527; b) B. Morgenstern, M. Michaelis, P. C. Baer, H. W. Doerr Jr., J. Cinatl, *Biochem. Biophys. Res. Commun.* **2005**, *326*, 905–908.
- [8] M. Wang, R. Cao, L. Zhang, X. Yang, J. Liu, M. Xu, Z. Shi, Z. Hu, W. Zhong, G. Xiao, *Cell research* **2020**, *30*, 269–271.
- [9] S. Adhikari, S. Meng, Y. Wu, *Infect. Dis. Poverty.* **2020**, *9*, 29.
- [10] M. Wang, R. Cao, L. Zhang, X. Yang, J. Liu, M. Xu, Z. Shi, Z. Hu, W. Zhong, G. Xiao, *Cell Res.* **2020**, *30*, 269–271.
- [11] M. Benucci, G. Giannasi, P. Cecchini, F. Li Gobbi, A. Damiani, V. Grossi, M. Infantino, M. Manfredi, *J. Med. Virol.* **2020**, *92*, 2368–2370.
- [12] a) L. J. Stockman, R. Bellamy, P. Garner, *PLoS Med.* **2006**, *3*, e343; b) N. Choudhry, X. Zhao, D. Xu, M. Zanin, W. Chen, Z. Yang, J. Chen, *J. Med. Chem.* **2020**, *63*, 22, 13205–13227.
- [13] a) D. Gurwitz, *Drug Dev. Res.* **2020**, *81*, 537–540; b) M. T. Kelleni, *Pharmacol. Res.* **2020**, *157*, 104874.
- [14] B. Shah, P. Modi, S. R. Sagar, *Life Sci.* **2020**, *252*, 117652.
- [15] K. Duan, B. Liu, C. Li, H. Zhang, T. Yu, J. Qu, M. Zhou, L. Chen, S. Meng, Y. Hu, C. Peng, M. Yuan, J. Huang, Z. Wang, J. Yu, X. Gao, D. Wang, X. Yu, L. Li, J. Zhang, X. Wu, B. Li, Y. Xu, W. Chen, Y. Peng, Y. Hu, L. Lin, X. Liu, S. Huang, Z. Zhou, L. Zhang, Y. Wang, Z. Zhang, K. Deng, Z. Xia, Q. Gong, W. Zhang, X. Zheng, Y. Liu, H. Yang, D. Zhou, D. Yu, J. Hou, Z. Shi, S. Chen, Z. Chen, X. Zhang, X. Yang, *PNAS* **2020**, *117*, 9490–9496.
- [16] Y. Liu, K. Wang, T. F. Massoud, R. Paulmurugan, *ACS Pharmacol. Transl. Sci.* **2020**, *3*, 844–858.
- [17] a) D. Musib, M. K. Raza, S. Kundu, M. Roy, *Eur. J. Inorg. Chem.* **2018**, *2018*, 2011–2018; b) K. H. Thompson, C. Orvig, *Dalton Trans.* **2006**, *6*, 761–764; c) D. Musib, S. Banerjee, A. Garai, U. Soraisam, M. Roy, *ChemistrySelect* **2018**, *3*, 2767–2775.
- [18] a) D. Musib, M. Pal, M. K. Raza, M. Roy, *Dalton Trans.* **2020**, *49*, 10786–10798; b) D. Musib, M. K. Raza, K. Martina, M. Roy, *Polyhedron* **2019**, *172*, 125–131.
- [19] S. Swaminathan, J. Haribabu, N. K. Kalagatur, R. Konakanchi, N. Balakrishnan, N. Bhuvanesh, R. Karvembu, *ACS Omega* **2019**, *4*, 6245–6256.
- [20] S. M. Chowdhury, S. A. Talukder, A. M. Khan, N. Afrin, M. A. Ali, R. Islam, R. Parves, A. A. Mamun, M. A. Sufian, M. N. Hossain, M. A. Hossain, M. A. Halim, *J. Phys. Chem. B* **2020**, *124*, 9785–9792.
- [21] M. Pal, D. Musib, M. Roy, *New J. Chem.* **2021**, *45*, 1924–1933.
- [22] A. Pandey, A. N. Nikam, S. P. Mutalik, G. Fernandes, A. B. Shreya, B. S. Padya, R. Raychaudhuri, S. Kulkarni, R. Prassl, S. Subramanian, A. Korde, S. Mutalik, *ACS Biomater. Sci. Eng.* **2021**, *7*, 31–54. 23.
- [23] R. Wang, J. Chen, K. Gao, Y. Hozumi, C. Yin, G. Wei, *Commun. Biol.* **2021**, *4*, 228.
- [24] D. S. N. B. K. Prasanth, M. Murahari, V. Chandramohan, S. P. Panda, L. R. Atmakuri, C. Guntupalli, *J. Biomol. Struct. Dyn.* **2020**, 1–15.
- [25] A. C. Walls, Y. J. Park, M. A. Tortorici, A. Wall, A. T. McGuire, D. Veessler, *Cell* **2020**, *180*, 1–12.
- [26] Y. Wang, Y. Wang, Y. Chen, Q. Qin, *J. Med. Virol.* **2020**, *2020*, 1–9.
- [27] X. Wang, W. Xu, G. Hu, S. Xia, Z. Sun, Z. Liu, Y. Xie, R. Zhang, S. Jiang, L. Lu, *Cell. Mol. Immunol.* **2020**, 1–3.
- [28] B. Tang, N. L. Bragazzi, Q. Li, S. Tang, Y. Xiao, J. Wu, *Infect. Dis. Model* **2020**, *5*, 248–255.
- [29] D. Wrapp, N. Wang, K. S. Corbett, J. A. Goldsmith, C.–L. Hsieh, O. Abiona, B. S. Graham, J. S. McLellan, *Science* **2020**, *367*, 1260–1263.
- [30] D. Guo, *Viol. Sin.* **2020**, *35*, 253–255.
- [31] a) A. Maxmen, *Nature* **2020**, *578*, 347–348; b) A. Ali, A. Pooya, L. Simani, *J. Neurol. Sci.* **2020**, *413*, 116832.
- [32] a) L. Zhang, D. Lin, X. Sun, U. Curth, C. Drosten, L. Sauerhering, S. Becker, K. Rox, R. Hilgenfeld, *Science* **2020**, *368*, 409–412; b) <https://www.rcsb.org/>.
- [33] Y. Gao, L. Yan, Y. Huang, F. Liu, Y. Zhao, L. Cao, T. Wang, Q. Sun, Z. Ming, L. Zhang, J. Ge, L. Zheng, Y. Zhang, H. Wang, Y. Zhu, C. Zhu, T. Hu, T. Hua, B. Zhang, X. Yang, J. Li, H. Yang, Z. Liu, W. Xu, L. W. Guddat, Q. Wang, Z. Lou, Z. Rao, *Science* **2020**, *368*, 779–782.
- [34] K. Das, S. E. Martinez, E. Arnold, *Antimicrob. Agents Chemother.* **2017**, *61*.
- [35] T. Marzo, L. Messori, T. Marzo, L. Messori, *ACS Med. Chem. Lett.* **2020**, *11*, 1067–1068.
- [36] M. Imran, M. Ramzan, A. K. Qureshi, M. A. Khan, M. Tariq, *Biosensors (Basel)*. **2018**, *8*, 95.
- [37] H. A. Rothan, S. Stone, J. Natekar, P. Kumari, K. Arora, M. Kumar, *Virology*. **2020**, *547*, 7–11 DOI: 10.1016/j.virol.2020.05.002.
- [38] M. Gil-Moles, U. Basu, R. Büssing, H. Hoffmeister, S. Türck, A. Varchmin, I. Ott, *Chem. Eur. J.* **2020**, *26*, 15140–15144.
- [39] D. A. Milenković, D. S. Dimić, E. H. Avdovićac, Z. S. Marković, *RSC Adv.* **2020**, *10*, 35099–35108.
- [40] W. A. Wani, E. Jameel, U. Baig, S. Mumtazuddin, L. T. Hun, *Eur. J. Med. Chem.* **2015**, *101*, 534–551.
- [41] J. Haribabu, S. Srividya, D. Mahendiran, D. Gayathri, V. Venkatramu, N. Bhuvanesh, R. Karvembu, *Inorg. Chem.* **2020**, *59*, 17109–17122.
- [42] T. M. Goszczyński, K. Fink, K. Kowalski, Z. J. Leśnikowski, J. Boratyński, *Sci. Rep.* **2017**, *7*, 9800.
- [43] N. Deng, S. Forli, P. He, A. Perryman, L. Wickstrom, R. S. Vijayan, T. Tiefenbrunn, D. Stout, E. Gallicchio, A. J. Olson, R. M. Levy, *J. Phys. Chem. B* **2015**, *119*, 976–988.
- [44] L. Zhang, D. Lin, X. Sun, U. Curth, C. rosten, L. Sauerhering, S. Becker, K. Rox, R. Hilgenfeld, *Science* **2020**, *368*, 409–412.
- [45] J. L. Thomaston, Y. Wu, N. Polizzi, L. Liu, J. Wang, W. F. DeGrado, *J. Am. Chem. Soc.* **2019**, *141*, 11481–11488.

Submitted: June 3, 2021

Accepted: July 20, 2021